Preprint of:

Berra F., Balini M., Levera M., Nicora A. and Salamati R. (2012) - Anatomy of carbonate mounds from the Middle Anisian of Nakhlak (Central Iran): architecture and age of a subtidal microbial-bioclastic carbonate factory. Facies (2012) 58:685–705, DOI: 10.1007/s10347-012-0299-z.

If interested, you can request the printed paper at **fabrizio.berra@unimi.it**

Anatomy of carbonate mounds from the Middle Anisian of Nakhlak (Central Iran): architecture and age of a subtidal microbial-bioclastic carbonate factory

Berra F.[1*], Balini M.[1], Levera M.[1], Nicora A.[1] & Salamati R.[2]

1. Università degli Studi di Milano, Dipartimento di Scienze della Terra "Ardito Desio", Via Mangiagalli 34, 20133 Milano, Italy
2. Geological Survey of Iran, Azadi Square, Meraj Avenue, 13185-1494, Tehran, Iran.

* corresponding author: e-mail: fabrizio.berra@unimi.it, tel. +00390250315498, fax +00390250315494

Abstract

The Anisian succession of Nakhlak (Central Iran) is characterized by a siliciclastic succession with minor carbonate intervals, with massive carbonate mounds up to 50 m thick in its upper part. These carbonate mounds, constrained in age to the late Bithynian (Ismidicus Zone) by ammonoids and conodonts, are characterized by a flat top and a lateral pinch out marked by clinostratified slopes (about 15° in dip). Stratigraphic and microfacies analyses document an inner part of the mound characterized by massive microbial carbonates with open-space structures (stromatactis) filled with fine-grained internal sediments and marine cements. Isolated sponges (up to 5 cm), serpulids and bryozoans are present, which grew on the calcimicrobial limestone. A narrow bioclastic margin (mainly with crinoids and brachiopods) produces most of the slope facies (consisting of bioclastic grainstone and packstone, with intraclasts from the inner part of the mounds) which interfinger basinward with volcaniclastic sandstones. The demise of carbonate productivity is marked on the top of the carbonate mounds by a condensed surface, rich in ammonoids, glaucony grains and articulated crinoids, documenting a rapid drowning. Palaeolatitude data support deposition in a tropical setting, and sedimentological constraints indicate deposition close to fair weather wave base, within the photic zone. The late Bithynian Nakhlak carbonate mounds developed before the appearance, documented since the Pelsonian in different parts of the world, of scleractinians which, despite the favourable environmental conditions, are absent at Nakhlak. The Nakhlak mounds thus represent one of the last occurrences of the microbial factories (which developed after the Permo-Triassic extinction event and persisted for most of the Middle Triassic, but with a gradually increasing role played by scleractinians) before the first appearance of the Mesozoic corals.

Keywords: carbonate mound, Anisian, Bithynian, ammonoids, conodonts, Central Iran.

1. Introduction

Marine carbonate production occurs in different environmental settings and in different ages with different features. Environmental conditions mainly control the nature of the marine carbonate factory (C-factories, T-factories and M-factories; Schlager 2003) whereas the carbonate-producing biota and the biogenic evolution mainly control the efficiency, morphology and production rates of carbonate factories through time. During the Phanerozoic, the most efficient carbonate factories are mainly developed in tropical settings and within the photic zone, where production is mainly related to metazoans (e.g. corals, sponges, molluscs), algae and bacteria (mainly cyanobacteria). The contribution of microbial vs. metazoan communities depends on the environmental-trophic conditions and on the metazoan associations developed in a specific time-interval of the history of the Earth. Factories mainly consisting of microbial carbonates are represented by carbonate mounds (M-factories *sensu* Schlager 2003) which are recorded in different climatic settings both at great water depth (below the photic zone) and within the photic zone. In shallow-water settings microbial carbonates generally prevail in a stressed environment, whereas in normal-marine settings they are commonly associated with carbonate produced by other organisms (i.e. corals) or abiotically (i.e. oolites).

The geological record is quite rich in examples of M-factories in the Palaeozoic, whereas their presence is less common in the Mesozoic and Cenozoic. Due to the nature of the carbonates, generally of microbial origin, the environmental interpretation of carbonate mounds is often challenging due to the lack of reliable bathymetric indicators and due to the difficulty of recognising both the organisms and the processes involved (Riding 2000). Deep-water carbonate mounds are generally characterized by a cone-shaped morphology which indicates their growth in quiet waters, with the top of the mounds below the zone of wave abrasion (i.e. below storm-weather wave base; Schlager 2003). Growth of massive microbial mounds is favoured in bathymetric levels where shallow-water, light-dependent, efficient carbonate-producing organisms were unable to live. Mounds developed below the photic zone are relatively abundant in the late Palaeozoic (i.e. Early Devonian Kess Kess mounds; Mounji et al. 1998; Wendt et al. 2001), whereas “Waulsortian mounds” (typical of Late Tournasian-Early Visean, in North America and central Europe; Flügel 2004) grew in tropical subphotic to shallow photic environments.

A few cases of microbial carbonates in tropical, shallow-water settings have been recorded, such as in the Fammenian succession of the Canning Basin, Australia (e.g. Playford 1984; Webb 2001). Shallow-water mounds are more common after major extinction events that affected the marine realm and in particular organisms involved in carbonate production (Schlager 2003), so that they generally occupy the ecological niches normally filled by tropical factories. In this context, carbonate mound production is mainly related to microbial activity, generally associated with cement-filled cavities (stromatactis) and bioclastic limestones, whereas the role of frame-building and baffling organisms is of minor importance.

In order to increase the knowledge of the distribution in time, morphological features and facies distribution of carbonate mounds, new and well-preserved case histories of different ages are needed. In the Anisian succession of Nakhlak (Central Iran, Fig. 1) a rare occurrence of shallow-water carbonate deposits within a mixed siliciclastic-carbonate succession is recorded. The detailed reconstruction of the facies and microfacies distribution allows a depositional model to be put forward and the depositional architecture to be defined for a relatively rare type of Middle Triassic carbonate factory, whose age is well-constrained by a rich palaeontological assemblage.

2. Geological setting

The Triassic in Iran is mainly represented by a carbonate succession which is characterized in its lower part (Early Triassic) by marly limestones and in its upper part (Middle-Late Triassic p.p.) by massive shallow-water dolomites (Seyed-Emami 2003). Two remarkable exceptions to this general stratigraphic setting are observed in north-eastern Iran (Aghdarband) and Central Iran (Nakhlak), where the Triassic succession is represented by volcaniclastic sandstones with intercalations of limestones and continental conglomerates (Alavi *et al.* 1997; Balini et al. 2009). Both successions have been interpreted as the result of deposition close to a volcanic arc generated by the northward subduction of the Palaeotethys ocean beneath the southern margin of Eurasia (Alavi *et al.* 1997; Balini et al. 2009; Muttoni et al. 2009; Zanchi et al. 2009), which lead to the Cimmerian Orogeny. The palaeogeographic location of these anomalous sections is still being debated. Soffel et al. (1996) suggested that Central Iran rotated counter-clockwise since the Triassic but the reliability of their palaeomagnetic data has been questioned recently by Muttoni et al. (2009).

The Triassic succession on Nakhlak, completely surrounded by desert sands (Fig. 1b), is stacked on hornblende metagabbros and silicified ultramafics south of Nakhlak along a low-angle fault. These rocks were interpreted as ophiolites by Holzer and Ghasemipour (1973), Alavi et al. (1997) and Bagheri and Stampfli (2008). The Triassic succession is strongly folded and faulted, so that tectonic repetitions occur, especially in the northern part of the area (Sharkovski et al. 1984; Zanchi et al. 2009). All the tectonic structures are unconformably sealed by Upper Cretaceous limestones (Sharkovski et al. 1984). The Upper Cretaceous and Paleocene beds are also deformed, showing an asymmetric anticline developed along an important north–south strike-slip dextral fault.

The Triassic succession of Nakhlak records three major intervals (lower marine, intermediate continental and upper marine) recorded by three formations (Davoudzadeh and Seyed-Emami 1972; Alavi et al. 1997; Seyed-Emami 2003; Balini et al. 2009): the first is the Alam Formation (Olenekian–Anisian; consisting of seven members, from A to G, Fig. 2), whereas the third, preserved only in the transgressive part, is represented by the Ashin Formation (Upper Ladinian). The intermediate continental episode is recorded by the Baqoroq Formation (Lower Ladinian).

Balini et al. (2009) provided a detailed and constrained reconstruction of the evolution of the succession, and documented a complex interaction between clastic–volcaniclastic supply and carbonate sedimentation, between regional subsidence and uplift, and between relative sea-level changes and syn-sedimentary tectonics and volcanic activity.

The base of the Alam Formation is not preserved, as it tectonically lies on metagabbro.

The Alam Formation is characterized by a transgressive part (from member A to member D, ‘nodular limestone’ of Balini et al. 2009), whereas the general regression is represented from member E to member G (‘grey shales’). The older unit (member A, ?lower Olenekian) was deposited in a coastal marine–transitional environment with input of fine-grained volcaniclastics with dissected–transitional arc provenance. Member B (‘oolitic limestone’; ?lower Olenekian), was deposited in a high-energy, shallow-marine environment and documents a rapid transgressive trend with a reduction of the volcaniclastic supply. The transgressive trend continues with the basal part of member C (Olenekian). Shales and siltstones increase in the upper part of member C (‘varicoloured shales’; middle–upper Olenekian). A decreased clastic input occurred before the deposition of the overlying member D (‘nodular limestone’, upper Olenekian), which was deposited in a deep-water environment. The transition from member D to the overlying thick member E (upper Olenekian-lower Bithynian) records a renewed, abundant volcaniclastic input related to a regressive trend which led to the onset of the carbonate mounds of member F (up to 50 m thick; Bithynian). The carbonate production of the mounds influenced sedimentation in the surrounding basinal areas, with deposition of an alternation of resedimented bioclastic intraclastic limestones and fine-grained sandstones. The carbonate mounds of member F represent the last important carbonate body preserved in the Nakhlak succession. The carbonate mounds, capped by hardgrounds with ammonoids, drowned in the late Bithynian, probably due to a very rapid sea-level rise, likely tectonically controlled (Balini et al. 2009). After a few meters of ammonoid-bearing marls (representing a deepening of the basin), the deposition of conglomerates and sandstones indicates the return to shallower-water facies (Member G; 'grey shales', upper Bithynian– Pelsonian or Illyrian). This unit reflects the progradation of coastal to alluvial facies intercalated with brackish-water lagoonal facies. The overlying Baqoroq Formation (up to 870 m thick; ?Upper Anisian–Ladinian), consisting of red conglomerates and sandstones, is referred to a fluvial environment in a semi-arid climate (Balini et al. 2009). In the Late Ladinian a new tectonic event led to the very fast transgression of the Ashin Formation, with the deposition of open-marine sediments (Balini et al. 2009). This fast environmental change was accompanied by renewed volcanic activity, documented by tuff layers up to a few metres thick.

3. The carbonate mounds of Nakhlak

The Alam Formation is characterized in its upper part by the occurrence of two coalescent carbonate bodies (member F) which reach a maximum thickness of about 50 m and have a present-day lateral length of a few hundred metres (Fig. 3). The Alam Formation shows reduced facies changes, suggesting deposition on a relatively homogenous sea-floor. These two coalescent mounds occur as isolated buildup in the eastern part of the succession, probably where even reduced changes in water depth and/or reduced siliciclastic input favored the onset of the carbonate production. The excellent conditions of the outcrop, the absence of pervasive tectonics and the generally well-preserved microfacies, as well as the high-resolution biostratigraphic control on the chronostratigraphic position of these mounds, allowed the careful characterization of the facies distribution and reconstruction of the environmental setting that favoured the development of the carbonate factory and controlled its demise.

Sampling was carried out mostly on the middle part and on the south-eastern margin of the carbonate bodies, where the boundaries with the underlying and overlying facies are best exposed. Four stratigraphic sections (Nakhlak 3, 4, 6 and 9: see Balini et al. 2009 for details) were sampled for lithofacies characterization and bio-chronostratigraphy (Fig. 3, 4). Sampling was performed to characterize both vertical (stratigraphic sections) and lateral facies change. From the collected samples, about 45 thin-sections were produced and described.

Twenty-four conodont samples were collected, together with about 130 ammonoids.

3.1. Chronostratigraphy of the mounds of Nakhlak

The chronostratigraphic position of the Nakhlak mounds is very well constrained by ammonoids and conodonts from the basinal facies (members E and G: Balini et al. 2009) underlying and overlying this carbonate body, as well as from the beds interfingering with the mounds (Fig. 4).

Ammonoids from the upper part of the Alam Formation were already reported by Davoudzadeh and Seyed-Emami (1972) and described by Tozer (1972). These specimens were not collected strictly bed-by-bed, but allowed the attribution of the member 4 of the

Alam Formation (*sensu* Davoudzadeh and Seyed-Emami 1972) to the Middle Anisian. Balini et al. (2009) reported for the first time conodonts from the middle part of the Alam Formation (members E and G), as well as bed-by-bed collected ammonoids.

The joint occurrence of ammonoids and conodonts in the Nakhlak succession supports an integrated bio-chronostratigraphy that is much robust than that based on a single tool. For the sake of chronostratigraphy, Triassic ammonoids and conodonts complement each other. The ammonoids provide high resolution dating because of the higher evolutionary rate of this group with respect to that of conodonts (cf. Balini et al., 2010). On the other hand, the medium power of resolution of conodonts is in part compensated by their higher frequency in the sedimentary record, then conodonts are often more practical than ammonoids for correlations.

Base of the mounds

The beds underlying the mound provided few ammonoids, but those obtained were of great bio-chronostratigraphic value.

At section Nakhlak 9, the levels NK430, NK433 and NK434 (Fig. 4 and 5) yielded respectively *Pseudodanubites* cf. *dritarshtra* Diener (Fig. 5a-b), *Kocaelia toulai* (Arthaber) (Fig. 5c-d) and *Nicomedites* sp. ind. (not figured: MPUM 10876 [NK434-2]). The genus *Pseudodanubites* in the Tethyan realm has been reported by Krystyn et al. (2004: fig. 8) from the middle Bithynian, with FO within the interval between the Caucasites and the Hollandites zones, and LO in the upper part of the Hollandites Zone.

Kocaelia is well constrained in its type area (Kocaeli peninsula, Turkey) where its FO is recorded in the very uppermost part of the Osmani Zone, then it ranges up to the top of the overlying Ismidicus Zone (Fantini Sestini 1988; 1990).

The occurrence of *Nicomedites*, marker of the Osmani Zone, from level NK434 a little above NK433, suggests the attribution of NK433-434 to the uppermost part of the Osmani Zone. As a result the basal part of the mound most likely is very lower Ismidicus Zone.
Conodonts have been recovered from both sections Nakhlak 3 and 9 (Fig. 6). In the lower part of the section Naklhak 3 an association of *Triassospathodus homeri* and *C. gondolelloides* has been found, indicating a late Olenekian age. About 75 m from the base of the section *Chiosella timorensis* along with *Neogondolella regale*, *Ng.* sp. A have been found, documenting the Aegean. Higher up, from 150 m from the base of the section up to the top (190 m), the conodont association is represented by *Neogondolella regale*, *Ng.* cf. *regale*, transitional forms *Ng. regale-Paragondolella bulgarica* and *P. bulgarica*. This fauna suggests a Bithynian age that is consistent with the age provided by ammonoids.
At section Nakhlak 9 the conodont sample NK435 yielded the association *P. bulgarica*-transition *P. hanbulogi* and *P. bifurcata*, while *Neogondolella* cf. *Ng. constricta cornuta* has been recovered in the sample NK436. According to Germani (2000) and Kovacs and Ralisch-Felgenhauer (2005) all of these forms occur from the lower Osmani Zone.

Top of the mounds

Ammonoids occur on the top surface of the mounds, in small marly limestone lenses immediately above the top and as isolated specimens from the overlying marls (Fig. 4, 7). The specimens from the top of the mounds are not extractable, whereas several ammonoids have been collected from the marly limestone lenses and the marls and tuffaceous marls at the base of section Nakhlak 6.
A very rich fauna dominated by “leiostraca” ammonoids *Sturia*, *Leiophyllites*, *Monophyllites*, but with also *Kocaelia toulai* (Fig. 7e-f) and very rare *Aghdarbandites* sp. has been collected from marly limestone lenses immediately above the top of the mound

(sample NK453). Four metres above sample NK453 *Aghdarbandites ismidicus* (Arthaber) Fig. 7c-d), together with *Gymnites asseretoi* Tozer (Fig. 7a-b) have been found from sample NK516. Being *Aghdarbandites* index of the Ismidicus Zone, the top of the mounds can be safely attributed to this zone, then to late Bithynian.

The conodont fauna found at the top of the mound along with the ammonoids (Fig. 4 and 6), is represented by *Gladigondolella malayensis* and transition *Ng. regale-P. bulgarica* (NK453) and by *P. bulgarica* from sample NK455. The occurrence of transition *Ng. regale-P. bulgarica* and *P. bulgarica* suggests a late Bithynian age for the top of the mound, that is perfectly consistent with the age demonstrated by ammonoids.

Correlations with other Anisian mounds

The Bithynian mounds of Nakhlak are the most accurately time-constrained Nakhlak mounds might be emphasized: the age with respect to the other Anisian mounds from the literature and their duration.

Chronostratigraphic correlation of the Nakhlak mounds with other known Anisian mounds suggests a partly overlapping age of the central Iranian mounds with respect to the Great Bank of Guizhou and the Anisian mounds of the western Tethys and the surrounding epicontinental seas. The rich ammonoid and conodont faunas of the Alam Formation surely demonstrate that the mounds from Nakhlak are older than most of the Anisian mounds from the western Tethys and the surrounding epicontinental basins, that since the XIX century have played a significant role in the understanding of the evolution of reef communities (e.g. Stanely, 2003). The appearance of carbonate mounds along the Tethys shelf, documented in Germany, Poland and Spain, as well as from the Northern and Southern Alps and Western Carpathians, is usually not bio-chronostratigraphically calibrated and it is referred to vaguely as Middle Anisian. The drowning of these mounds in the late Pelsonian (latest Middle Anisian) or Illyrian is often well calibrated by ammonoids and/or conodonts from the overlying basinal facies. In the Western Tethys, only the Monte Rite Formation (the Dolomites: Neri et al, 2007; Stefani et al., 2010) is probably Bithynian in age, as Pelsonian faunas have been observed on condensed surfaces on its top.

Very important are the time-correlations with the Anisian reef of Great Bank of Guizhou, that has become famous in the last 15 years as the first reef of the Anisian (e.g., Lehrmann et al. 1998, Payne et al. 2006a, 2006b). The onset of the development of the reef is probably earlier in Guizhou with respect to Nakhlak, but accurate comparisons are difficult because the timing of the development of the Anisian reef of the Great Bank relies only on conodonts (Orchard et al. 2007) collected from basinal facies (Lower and Upper Guandao sections) correlated to the reef over a distance of at least 1 km, but not directly underlying or overlying it (see Payne et al. 2006a). Another feature that does not help the correlations is the faunal difference of the Guandao sections with respect to Nakhlak. At the Guandao sections (Orchard et al., 2007) the conodont distributions show two main unusual ranges. The first is the overlap of *Chiosella gondolelloides* with *C. timorensis* and its longer range in respect of *C. timorensis*. Whereas the second is the occurrence of these two species in the Bithynian together with *Nicoraella germanica* and in early Pelsonian along with *Nicoraella kockeli*. In the Tethyan realm, the latter two species are usually found in the late Bithynian and Pelsonian respectively, but never occur together with *C. timorensis* and *C. gondolelloides*. The group consisting of *Neogondolella regale*, *Paragondollella bulgarica* and their transitional forms, rather common in the Bithynian of Nakhlak, has not been identified at Guandao.

The last peculiar feature of the Nakhlak mounds is their very short duration. Accepting a very late Osmani Zone age for its base and an Ismidicus Zone for its top, the maximum duration of the mounds is one ammonoid zone, but it might be even less. Such a figure would mean a carbonate production rate of about 50 m per ammonoid zone: the calculation of a reliable production rate vs. time is highly speculative because the duration of the ammonoid zones is not well-constrained and thus any calculation would suffer a very large approximation, as the error is larger than the duration of an ammonoid zone. Nevertheless, it is possible to suggest a relatively high production rate on a short time interval.

3.2. Depositional architecture of the mounds: sedimentology and facies distribution

The carbonate mounds have a relief estimated to have been at least 30 m above the surrounding basinal facies and they interfinger basinwards with an alternation of limestones, resedimented from the mounds, and fine-grained siliciclastics. The top of the mounds is connected to the basinal sea-floor along a clinostratified slope with angles of about 10-15° (Fig. 3). Normal grading (in the carbonates) and parallel to hummocky stratification are common in the transitional area between the slope of the carbonate mound and the basinal succession. Limestone content increases toward the carbonate mounds and the clastic component is reduced to thin layers between the calcareous beds (Fig. 8 a, b). Limestone beds become rapidly coarser toward the upper part of the slope, where large crinoid ossicles are common (Fig. 8c). Here, beds are more massive and cross-laminations are common (Fig. 8d). The core of the mound, where bedding is absent, is composed of massive limestones with large (up to about 10 cm) cavities which are filled by internal sediments or by cements (Fig. 8 e, g). Sponges and bryozoans are commonly found in these massive limestones (Fig. 8 f). The carbonate mounds are bounded at the top by a flat surface (Fig. 8h) that marks the end of the carbonate production. On this surface, abundant ammonoids, crinoids (it is common to observe long fragments of articulated crinoid ossicles) and phosphatic crusts are present, later covered by marls and volcaniclastic sandstones.

Two coalescent mounds can be recognized. They are separated, in the marginal part, by a tongue of limestones and fine-grained sandstones, but tend to amalgamate in the innermost part.

These carbonate mounds represent isolated carbonate bodies that intercalate in a prevailing volcaniclastic succession. Whereas the lateral transition between the mounds and the siliciclastics is gradual, the sharp upper boundary of the mounds is indicative of a rapid change in the depositional environment, related to a rapid drowning.

3.3. Facies types

On account of the sedimentological structures, microfacies composition (both bioclastic and inorganic) and texture, seven facies have been identified within the mounds. These facies (F1 to F7 in Fig. 9) define the different parts of the mounds:

F1 – Encrinites: bioclastic calcarenites mainly consisting of crinoid ossicles (up to 1.5-2 cm in size) and a minor amount of echinoid fragments (Fig. 10a). The intergranular space is generally represented by micrite (packstone), only rarely by cements (grainstone). Other grains are represented mainly by bioclasts (bivalves) or intraclasts. Rare volcanic fragments are present. Bioclasts indicate a reduced level of reworking. Locally normal grading has been observed; bedding ranges from 2 to 15 cm in thickness. A low-angle clinostratification is observed.

F2 – Bioclastic packstone: grains mainly consist of fragments of crinoids, echinoids, bivalves, gastropods, brachiopod, bryozoans and green algae, in different percentages (Fig. 10b). Intraclasts are locally present, together with extrabasinal volcanic fragments. Reworking of the bioclasts is generally high: gastropods and bivalves are often characterized by mechanical erosion and are rounded (Fig. 6b). Locally, cross stratification is common; beds are generally a few centimetres thick.

F3 – Intraclastic packstone: the grains are mainly represented by clasts of microbial carbonates, often with a clotted texture (Fig. 10c, d). Bioclasts generally represent less than 40% of the grains and mainly consist of bryozoans, bivalves, crinoids and rare foraminifera. Volcanic grains are rare.

F4 – Bioclastic-extraclastic wackestone: intraclasts and bioclasts (echinoderms, bivalves and brachiopods) float in a fine-grained calcareous matrix, locally rich in small lithic volcanic fragments (Fig. 10e). Foraminifera (*Nodosariidae*) are present. Bedding is generally parallel.

F5 – Calcimicrobial limestone (Fig. 11): this consists of massive clotted framestone, characterized by open-space structures (stromatactis) filled with fine-grained internal sediments or marine cements. The latter, on account of the black colour in cathodoluminescence (Fig. 11g, h), can be interpreted as early marine cements. Thrombolitic macroscopic clotted fabric is typical. In thin section it is locally possible to identify a *Renalcis*-type globular calcified cyanobacterial framework (Fig. 11c), consisting of irregular masses of thick-walled reniform chambers, partly filled with micrite or cements. Assemblages of irregular thin-walled cells filled with calcite building cm-sized elements in the calcimicrobial limestones can be referred to as *Bacinella* (Fig. 11d). Other encrusting mats of different types are present, indicating a rich assemblage of calcimicrobes and problematica, contributing to the carbonate production of the mounds. Within the massive clotted framework, large isolated sponges (up to 5 cm in diameter, Fig. 8f), ostracods, serpulids and bryozoans are present. Bryozoans and serpulids commonly grow on the irregular morphology of the calcimicrobial limestone, often colonizing cavities within the mound. These organisms are commonly enveloped by microbial mats. The growth of sessile organisms in cavities of the calcimicrobial limestone indicates development of a rigid framework (Fig. 11a, b, c) where a complex net of cavities was present. The microbial origin of the sediments controlled the firmness of the carbonate, which represented a favourable substrate for the growth of the sessile organisms (Fig. 11e). The presence of organisms within these cavities indicates a connection of the cavity network with the sea-floor. The cavities are eventually filled by fine-grained internal sediments and/or cements. Echinoids and brachiopod fragments are locally present, mainly close to the transition with the encrinites and bioclastic packstone facies. The overall aspect is massive. Thin layers of packstone and grainstone with microbial and skeletal grains (mainly brachiopods and crinoids) locally intercalate within the microbial limestone, suggesting a partial erosion and local reworking of the sediments of the calcimicrobial facies during episodes of higher energy.

F6 – Sandy limestone: this consists of wackestone with a calcareous matrix and abundant fine-grained, quartz-rich volcanic material, with sparse bioclasts (Fig. 10 f, g). Bioclasts are represented by thin-shelled bivalves, brachiopods, crinoid ossicles, ostracods and bryozoans.

F7 – Fe-rich mudstone-wackestone: wackestone with dispersed abundant ammonoids, crinoid ossicles (partly still connected), ostracods and rare bryozoans and sponges. Rare small volcanic grains (mainly quartz) are present. Glaucony grains are rare. This microfacies represents a thin layer that covers microfacies 5. Fe-rich crusts characterize these horizons.

3.4. Depositional model

The association and distribution of the seven facies within the carbonate mound defines a complex depositional environment. On account of the facies association and the sedimentological processes that controlled both the carbonate production and the sediment distribution, the carbonate mound can be divided into the following sub-environments.

Inner part of the mound (microbial buildup): this part is exclusively represented by microfacies 5. The homogeneous distribution of the calcimicrobial limestones indicates that they were produced *in-situ*, without important sedimentological contribution from the margins of the mounds, that were characterized by different facies. Calcimicrobial limestones formed a rigid framework which represented the substrate for the growth of bryozoans, sponges and serpulids (Fig. 11b, c), which were also enveloped in the microbial mats (Fig. 11a). The growth processes of the calcimicrobial mound favoured the development of abundant open-space structures, later filled with fine-grained internal sediments (crystal silt, Fig. 11b, e) or early, marine abiotic cements (Fig. 11c, f, g). The cavities (generally less than 1 cm across, but locally up to 5-10 cm in size) were formed during the growth of the mound, as indicated by the presence of serpulid tubes and bryozoans that grew on the walls of the cavities. The presence of organisms indicates that the network of cavities was connected to the depositional surface. The calcimicrobial mound can be considered, at least partially, as a framestone (*sensu* Lehrmann 1999), even if not constructed by large frame-building metazoans.

The facies association indicates persistent subtidal conditions and no evidence for subaerial exposure of the mound has been observed. The presence of a flat top is unlikely in deep-water mounds, where a conical shape of microbial mounds is common (e.g. Wendt et al. 2001; Schlager, 2003): the presence of a flat top is therefore indicative of a process that prevented the conical growth of the mounds, but was not related to subaerial exposure. The nature of the carbonate-producing organisms does not permit the palaeo-water depth to be constrained; nevertheless the possible presence of *Renalcis* (a phototrophic cyanobacteria) and *Bacinella* is compatible with deposition within the photic zone, as has been observed in carbonate mounds of different ages. Microbial associations, along with the bathymetric constraints from the upper part of the Alam Formation, indicate that the morphology of the top surface of the mound was probably related to erosion within the zone of wave action and that the continuous effect of normal wave action on this elevated area (with respect to the surroundings) prevented the carbonate factory from catching up to the sea-level surface; hence the flat top of the mound was maintained within the photic zone. The top of the mound was likely controlled by the fair-weather wave base whereas, according to this interpretation, the sea-floor in the basinal area was deeper that the fair-weather wave base (likely close to the storm-weather wave base, as evidence of sediment reworking by wave activity is scarce).

"Margin": the massive inner part of the mound laterally passes to bioclastic packstone and, less frequently, grainstone, particularly rich in crinoid ossicles (facies F1 and F2). The transition from the inner part of the mound tothe "margin" facies is relatively rapid. The occurrence of large skeletal grains in the "margin" is indicative of a high energydepositional setting, suggesting deposition in a wave-washed setting. The distribution of the bioclastic limestones indicates a decrease in abundance and size according to bathymetry, from the platform top to the clinostratified slope. Bioclastic production was mainly concentrated at the boundary of the inner platform, where crinoids, associated with brachiopods, were present. The abundance of crinoids is indicative of normal-marine conditions. The reworking of the bioclastic debris toward the slopes of the mound and, in minor quantity, toward the inner platform resulted from the activity of waves on the crinoid meadows, that were destroyed during severe storms. Reworking of the inner part of the mound is documented by the occurrence of microbial intraclasts along the slope. High-energy events were therefore able to deliver material from the inner mound to the slope, giving rise to deposits composed of bioclasts and intraclasts (facies F3 and F4).

The rims of the mounds therefore represent the areas of production for most of the skeletal grains and a permeable barrier between the inner mound and the slopes. The continuity of the margin was probably interrupted by channels/inlets which favoured the delivery of the microbial intraclasts from the microbial mound to the slopes, where they were mixed with the “margin”-derived skeletal grains.

Slopes: the massive bioclastic facies rapidly evolves to clinostratified bioclastic packstone in beds up to 15-20 cm thick, commonly amalgamated. Facies mainly consist of type F1, F4 and, less frequently, F6. Normal grading is common. Beds are clinostratified, with an angle of about 10-15°. The slope angle is controlled by the grain size of the deposits, as early cementation, which is common in slope and margin facies of other platforms in the geologic record, does not significantly favour the stabilization of the slopes. Also the production of microbial limestones on the slope is not documented; calcimicrobial limestones occur only as clasts, probably derived from the inner part of the mound during rare high-energy episodes (i.e. storm events). The length of the clinoforms is not well constrained, but it probably reaches some tens of metres.

Basinal facies: the distal part of the clinoforms interfingers with sandy limestones rich in volcanic fragments. The clastic material is less abundant with respect to both the succession underlying and overlying the mounds, suggesting a minor clastic input to the basin during the deposition of the carbonate mounds. Far from the mounds, the bioclastic content decreases. Facies mainly consist of type 6 and 7.

Facies distribution, coupled with the external geometry, has allowed the reconstruction of the depositional architecture of the carbonate mounds of Nakhlak (Fig. 12). Field evidence points to a high relief microbial mound, characterized by a flat top and a bioclastic margin where crinoids and brachiopods dominate. The sediments derived from the margin (and, in minor amount, from the inner mound) were mostly transported toward the basin, leading to the development of a clinostratified slope (about 30 m high) which laterally passed to basin-floor limestones and volcaniclastic sandstones. Resedimentation along the slopes favoured the interfingering of graded bioclastic-intraclastic limestones within the fine-grained siliciclastic basinal deposits. Interruption in the continuity of the bioclastic marginal area favoured the deposition of skeletal grains toward the inner part of the mound and, at the same time, the sedimentation of intraclasts from the inner mound along the slopes. The sharp top of the mound, coupled with the condensed deposits of facies F7, favoured the preservation of the original geometry of the carbonate mound, at least along an E-W oriented section. The flat top is likely the result of wave abrasion on the inner mound, which maintained its top close to fair-weather wave base. The intense reworking of the sediments (as documented by abundant well-rounded skeletal grains) can be thus ascribed to wave activity on the highest parts of the mound.

4. Discussion

4.1. Anatomy of the Nakhlak carbonate factory

The facies distribution within the Anisian mounds of Nakhlak indicates the existence of two major different sources of carbonate within the factory which are related to two different sub-environments (Fig. 12). The first and volumetrically dominant was represented by a "mud" factory that produced fine-grained massive biotically-induced limestones, with open-space structures that were firm or hard upon formation, as documented by the microfacies textures. This microbial/mud factory represented a favourable environment for bryozoans, serpulids and sponges, which colonized and encrusted the firm surfaces of the microbial limestones. The second factory ("margin" factory) is mainly skeletal and represented by crinoidal meadows that developed at the rims of the microbial/mud factory.

Whereas the carbonate produced by the microbial/mud factory is mainly preserved *in situ*, the nature of the "margin" factory is mainly documented indirectly, by the composition of the slope facies which mainly consist of crinoidal packstone. A minor contribution to carbonate production was provided by other organisms: sponges, bryozoans and serpulids in the "mud" factory whereas bivalves, brachiopods and gastropods lived together with the crinoids in the "margin" factory and are preserved in the slope facies.

The "margin" factory was developed only at the rims of the mound and was not able to spread towards the inner part, as documented by the rare occurrence of crinoid ossicles in the inner part of the mound. The reduced mixing of sediments from the "margin" and from the microbial/mud factory supports a well-defined distribution of the different types of carbonate producing biota in the mound, probably reflecting different palaeoecological conditions in the inner part of the mound and along the margin. The abundance of crinoids on the hardground surface at the top of the mound suggests that the growth of the mound ended with a crisis for the "mud" factory which favoured the spread of crinoids on to the top of the mound.

The relief of the mound was likely around 30 metres. The transition with the underlying resedimented limestones and volcanics is sharp, as sharp as the top of the mound. The mechanism that induced the development of the mound during the Bithynian should be favoured by a decreased input of siliciclastics and to the regressive trend of the Alam Formation (Balini et al., 2009). Due to the regressive trend the sea-floor probably reached a favourable depth for the inception of the microbial/mud factory and, thus, for the development of the mounds. The end of the mound evolution, marked by a hardground covered by clastic deposits, is likely related to a relative sea-level rise.

The question is why a relative rise of sea-level did stop both the microbial/mud and the "margin" carbonate factories. The geometry of the mound, the microbial assemblage and the presence of sedimentary structures indicate that carbonate production occurred at depths that were likely comprised between the fair-weather and storm-weather wave base. Therefore, the top of the mound was within the photic zone, so that the microbial carbonate production was favoured by light-dependant microbial associations. In these conditions, a rapid relative sea-level rise of a few tens of metres likely moved the top of the mound from the photic to the non-photic zone, halting the microbial activity. At these depths, crinoids were able to conquer the top of the mound, but the skeletal production was not sufficient to recover the relative sea-level rise. The top of the mound became a condensed surface, only later covered by renewed clastic input that gradually smoothed the basin floor (first covering the basinal area, then the top of the mound), eventually leading to a shallowing of the basin until continental conditions in the uppermost part of the Alam Formation, some tens of metres above the top of the mound.

4.2. Significance of the carbonate factory

The Anisian carbonate mounds of Nakhlak represent a particular event of carbonate production, exceptionally constrained in age, during the early Mesozoic. The favourable outcrop conditions and the well-preserved geometries and microfacies allowed the detailed description and reconstruction of the geometry of the mounds and of their depositional setting. Their features closely resemble those of Palaeozoic mounds (Devonian, e.g. Shen et al. 2008 and references therein), but also of the Early Triassic mounds of Southern China (Lehrmann 1998; 1999). The Anisian part of the Chinese mounds show some similarities (abundance of microbial carbonates with *Tubiphytes*, with crinoids that dominate the skeletal component, followed by bivalves) with the Nakhlak mounds. Nevertheless, the platform is larger and thicker (about 600 m of late Smithian-Anisian

carbonates) and there are differences in the facies distribution: in the inner part of the carbonate platform the presence of lagoonal and peritidal facies (completely missing at Nakhlak) is documented, whereas breccias are commonly observed on the slopes (Payne et al., 2006b). The observed association of sponges and microbialites in Nakhlak is not describe in the Anisian mounds of China, but is similar to that reported by Hips (2007) in the Middle Anisian of Hungary. The presence of bryozoans, occurring at Nakhlak, is reported from the Anisian Monte Rite Formation in the Dolomites (Stefani et al., 2010), but in this latter platform the presence of dasycladacean algae highlights a difference in the carbonate-producing biota with respect to Nakhlak. The first Mesozoic occurrence of various sponges and serpulids associated with microbialites and other eukaryotic benthic organisms is reported in reefs from the Western USA only 1.5 million years after the Permo-Triassic extinction event (Brayard et al., 2011) suggesting that the recovery of carbonate production was relatively rapid, but with communities without scleractinians.
The deposition of the Nakhlak mounds likely occurred in tropical settings, as indicated by the occurrence of oolitic limestones in the lower part of the Alam Formation and by the palaeolatitudinal position of the Nakhlak succession (palaeomangetic data indicate a latitude of 21°N ±4° in the upper Olenekian; Muttoni et al. 2009). The climatic and bathymetric conditions were thus favourable for the development of T-factories *sensu* Schlager 2003; nevertheless corals are absent. The absence of scleractinian corals associated with the carbonate mounds cannot be ascribed to the environmental conditions or water depth, as the mounds of Nakhlak were formed in warm waters at a depth close to the base of the fair weather wave base, neither to the trophic conditions, as corals are often associated with similar microbial limestone in slightly younger Middle Triassic reef facies of the Tethys (e.g. Senowbari-Daryan et al., 1993; Keim and Schlager 2001). Therefore, the reason for the absence of scleractinian corals can be confidently ascribed

to the fact that the development of the mounds of Nakhlak predated the appearance of Mesozoic scleractinian corals after the P-T biologic crisis, which is responsible for the absence of the typical T-factory fossil assemblages in the Early Triassic and part of the Anisian (e.g. Flügel and Stanley 1984) during a time interval of about 14 Ma according to Stanley (2003), but probably less (about 10 Ma according to Mundil et al., 2010). The contribution to carbonate production by scleractinians was reduced during Anisian times, gradually increasing through the Ladinian until they became very important carbonate producers during the Late Triassic, with a peak during the Norian (Kiessling 2010).

The precise date of the appearance of scleractinians during the Middle Triassic relies both upon the oldest appearance of corals and on the youngest occurrence of carbonate factories with environmental conditions favourable for the growth of scleractinians, but without them. The oldest corals described in the Triassic limestones of Tethys are dated at the Pelsonian (Morycowa 1988; Senowbari-Daryan et al. 1993; Berra et al. 2005), and a possible specimen of a scleractinian coral was observed higher in Pelsonian strata by Payne et al. (2006b) in Southern China (Great Bank of Guizhou). Despite the absence of scleractinians, carbonate buildups are present also before the Pelsonian. Carbonate production was mainly related to chemical precipitation (oolites) or calcimicrobial activity (carbonate mounds) and accumulation of bioclastic debris. These buildups strongly differ from larger and younger Mesozoic buildups, where an increasing role in carbonate production is played by metazoans and the role of calcimicrobes decreases. The dominant role of calcimicrobial limestones in the Early Triassic and part of the Anisian is never observed in younger successions, where calcimicrobial production, locally important, gradually decreases its importance until it becomes an accessory to more complex carbonate-producing biotic associations. In the Early Triassic and part of the Anisian, the M-factories provide most of the shallow-water carbonate production even at tropical latitudes, building high-relief mounds rimmed by oolitic sands (as in the case of the Great Bank of Guizhou; Lehrmann 1999) or by crinoidal-debris margins (as in the case of the Nakhlak mounds). The appearance of scleractinian corals since the Pelsonian gradually reduced the role of "pure" M-factories (dominant at the beginning of the Triassic, immediately after the Permo-Triassic extinction) from shallow to deeper water, as the carbonate M-factories slowly evolved, in tropical settings, to rimmed T-factories (*sensu* Schlager 2003) which will increase their role through the Triassic.

The absence of scleractinians in a favourable environment such as that of the mounds of Nakhlak strongly supports the hypothesis that this carbonate factory developed before the appearance of the Mesozoic corals, thus allowing the framing of their appearance in the time interval between the drowning of the Nakhlak mounds (Late Bithynian, *A. ismidicus* Zone) and the first documented occurrence of corals in the Pelsonian.

5. Conclusions

M-factories in shallow-water and in tropical settings are unusual in the geological record. Their presence is generally ascribed to the absence of competitive, more efficient, carbonate factories, because of environmental conditions or major extinctions (Riding and Liang, 2005). The geometry and facies distribution of well-preserved carbonate mounds, characterized by high relief and the presence of two different major sources of carbonate have been reconstructed in the Anisian succession of Nakhlak (Central Iran). The chronostratigraphic position of these carbonate mounds is exceptionally well-constrained by the presence of ammonoids and conodonts at the late Bithynian (within the *A. ismidicus* Zone). In the Late Anisian mounds of Nakhlak carbonate production occurred as a) microbial limestones in the inner part of the mound and b) skeletal (mainly crinoid) grains, which build clinoforms, in the marginal area of the mound. The carbonate facies, interfingering with mixed carbonate-siliciclastic deposits basinward, are capped by a condensed surface which marks a crisis for the carbonate factory. The geometry of the mound is ascribed to wave abrasion on its flat top.

Environmental conditions were favourable for the growth of T-factory biotic associations, but scleractinians are absent, supporting the hypothesis that the growth of the mound of Nakhlak closely predates the first appearance of Mesozoic corals, whose presence is documented in different M-type carbonate factories in the Pelsonian. These mounds are among the youngest tropical M-factory of the Triassic where sclearactinian are absent, and they represent the last “pure” M-type Triassic carbonate factories before the slow and gradual transition of carbonate production toward T-type factories, due to the appearance of the scleractinians. The presented data on the Nakhlak mounds therefore frame the appearance of scleractinian (and thus the beginning of the gradual shift toward typical T-factory Mesozoic reefs) in a time interval comprised between late Bithynian (*A. ismidicus* Zone) and Pelsonian, constraining the recovery intervals of corals after the Permo-Triassic extinction. These results indicate that the appearance of scleractinians can be framed in a well-defined time interval of the Middle Triassic, so that it is possible to focus the attention exactly on this time interval in order to try to understand how and why scleractinian, among the most important carbonate producers from the Mesozoic to the Holocene, appeared.

Acknowledgements

Fieldwork was funded by the MEBE projects ‘Stratigraphy of Selected Permian and Triassic Sections in Iran’ (leader M. Gaetani) and ‘Tectonic Evolution of the Yazd, Tabas and Lut Blocks (Central Iran) by Means of Palaeomagnetic, Structural and Stratigraphic Data’ (leader M. Mattei) in cooperation with the Geological Survey of the Islamic Republic of Iran. This work has been possible thanks to the fundamental support of Dr. M.R. Ghassemi and Dr. A. Saidi of GSI that are here warmly thanked. M. Mattei, G. Muttoni and

A. Zanchi are thanked for support during field work. The paper benefitted from the careful comments of two anonymous reviewers and from the helpful suggestions of the Editor M. Tucker. Special thanks also to the administration and the miners of the Nakhlak Mining Company for their kindness and hospitality. Technical support for the conodont study was kindly provided by Irene Vuolo.

Figure captions

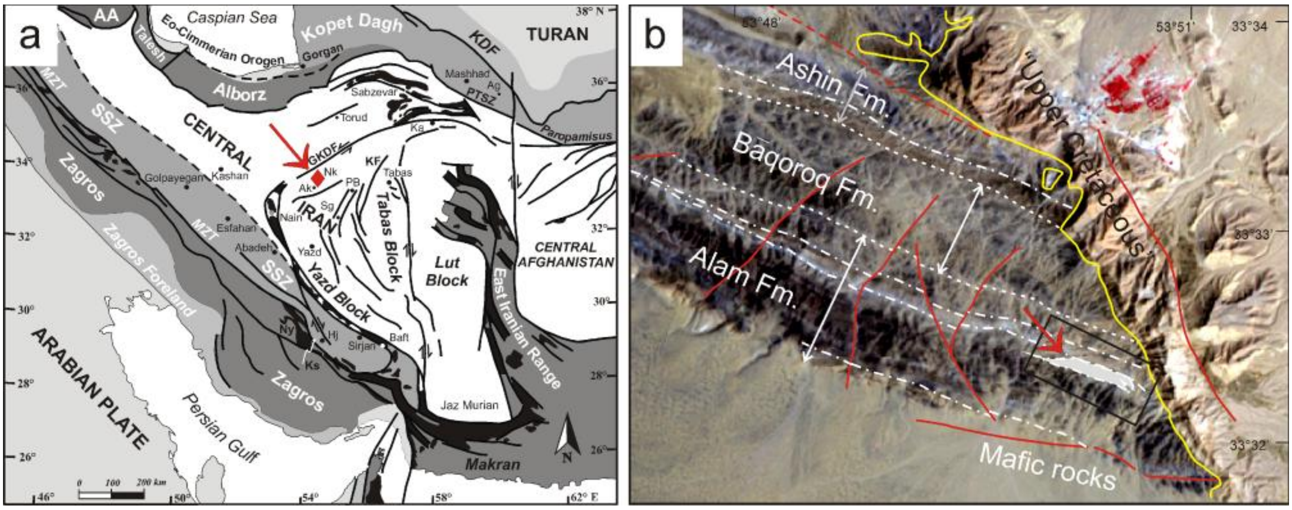

Fig. 1 – Location map of Nakhlak (Central Iran) on a structural model of Iran (from Angiolini et al. 2007). (a; arrow points to the Nakhlak succession) and satellite image (ASTER; b) of the Nakhlak area, with lithostratigraphic boundaries of Triassic units (white dashed line), angular unconformity with the Cretaceous sediments (yellow line), major faults (red lines) and position of the studied carbonate mounds (box).

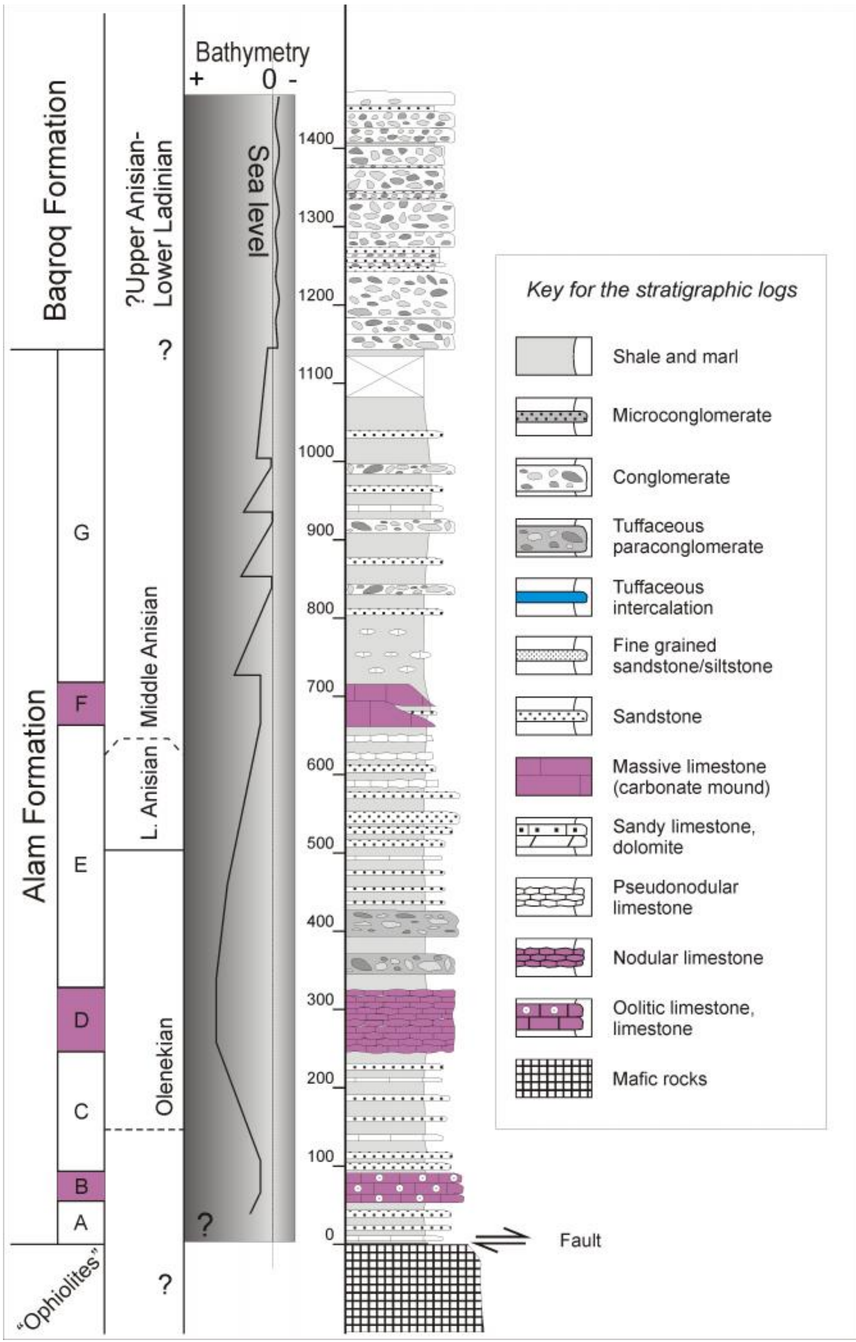

Fig. 2 – Composite geological section of the Alam Formation and part of the overlying and underlying succession (modified after Balini et al. 2009). Detailed description of the lithostratigraphic units is provided by Balini et al. 2009, member F corresponds to the carbonate mounds.

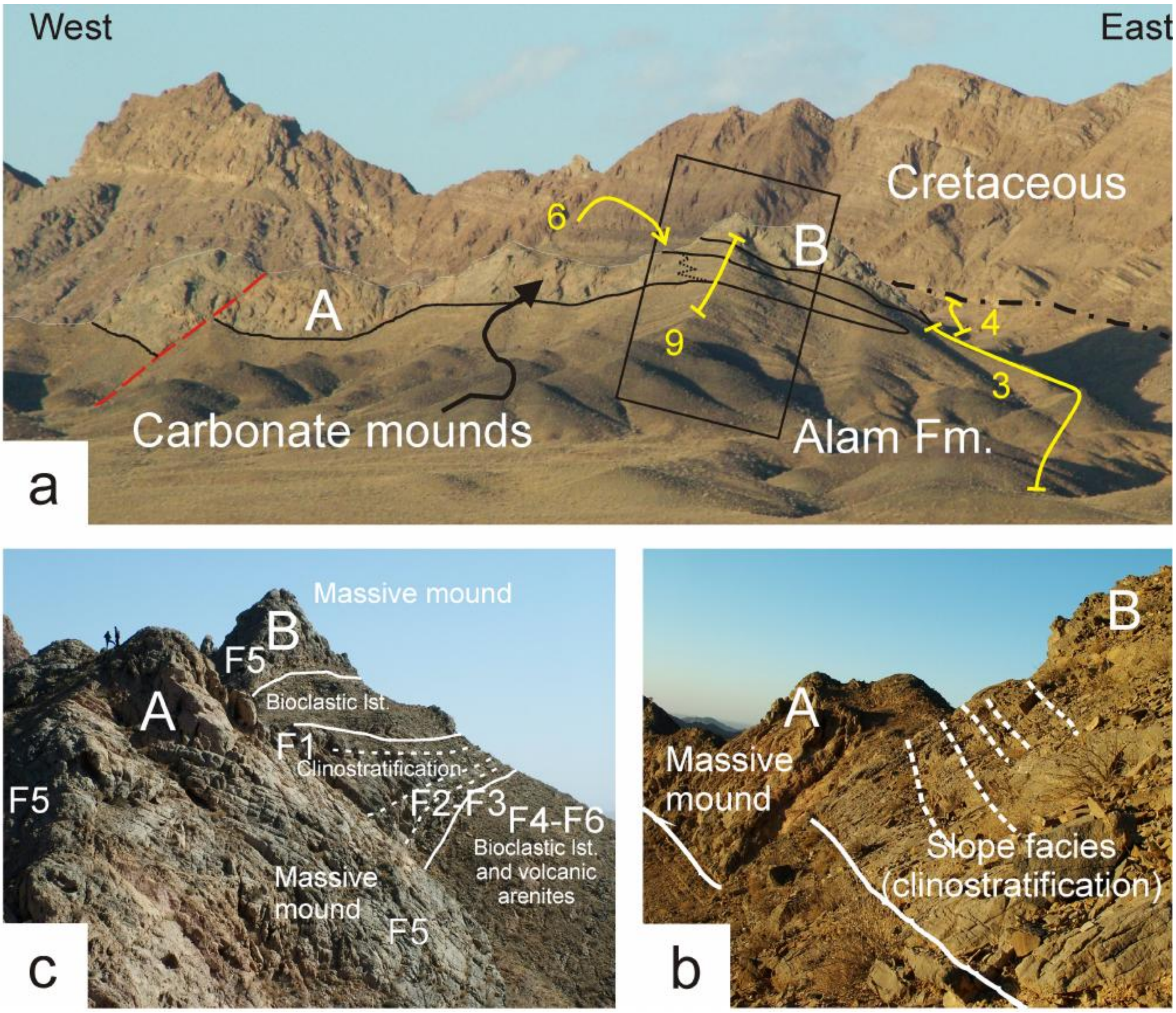

Fig. 3 – a) Panoramic view of the Kuh-e-Qal'eh Bozorg from the SW. A and B refer to the two coalescent carbonate mounds, numbered lines mark the position of the stratigraphic sections Nakhlak 3,4,6 and 9 of Fig. 4; b) detail of the box in Fig. 3a view from the west: note the lateral closure of mound A toward the right along a clinostratified slope, before the progradation of mound B (F1 to F6 refer to the facies described in the text and in Fig. 9); c) detail of the box in Fig. 3a view from the east (from basin to the carbonate mound).

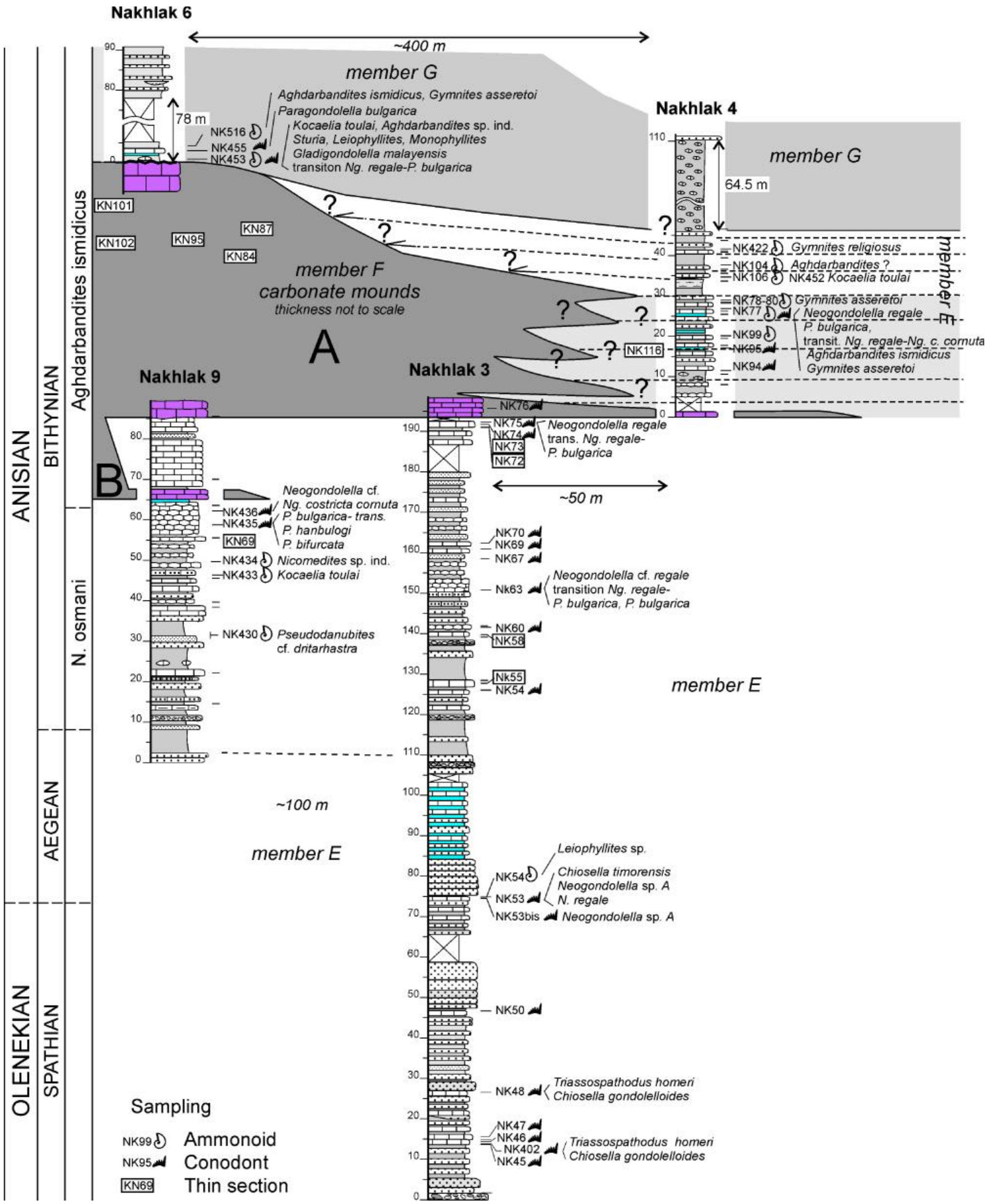

Fig 4 Detailed stratigraphic framework of the Anisian mounds of the Alam Formation, based on four bed-by-bed sampled stratigraphic sections Nakhlak 3,4,6 and 9 (Balini et al. 2009). The position of all the studied samples, including lithofacies characterization, macro and microfossils for bio-chronostratigraphy is shown. For the description of lithostratigraphic units see Balini et al., 2009.

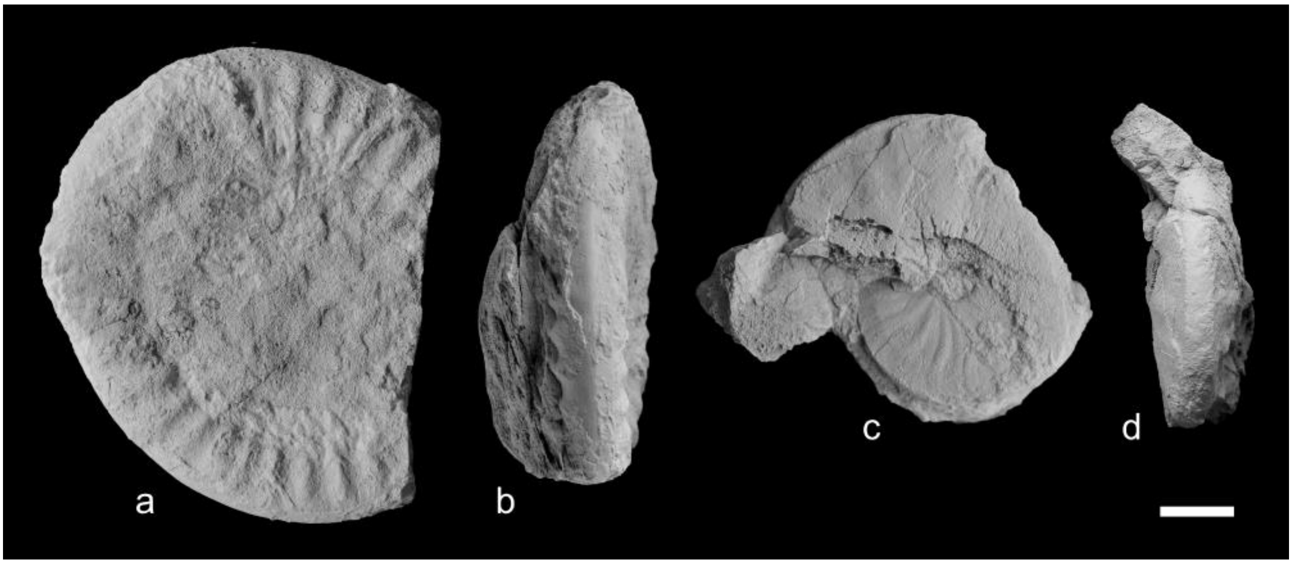

Fig. 5 Early Bithynian ammonoids from the Alam Formation, member E, Nakhlak 9 section, *Nicomedites osmani* Zone. See Fig. 4 for stratigraphic position of the samples. **a**–**b** *Pseudodanubites* cf. *dritarashtra* (Diener 1895), MPUM 10874 (NK430-1). **a** lateral view; **b** ventral view. **c**–**d** *Kocaelia toulai* (Arthaber 1914), MPUM 10875 (NK433-1), specimen with test. **c** lateral view; **d** ventral view. Bar scale 1 cm. The specimens are housed at Museo di Paleontologia of Dipartimento di Scienze della Terra "Ardito Desio", University of Milano. The repository number (MPUM) is given.

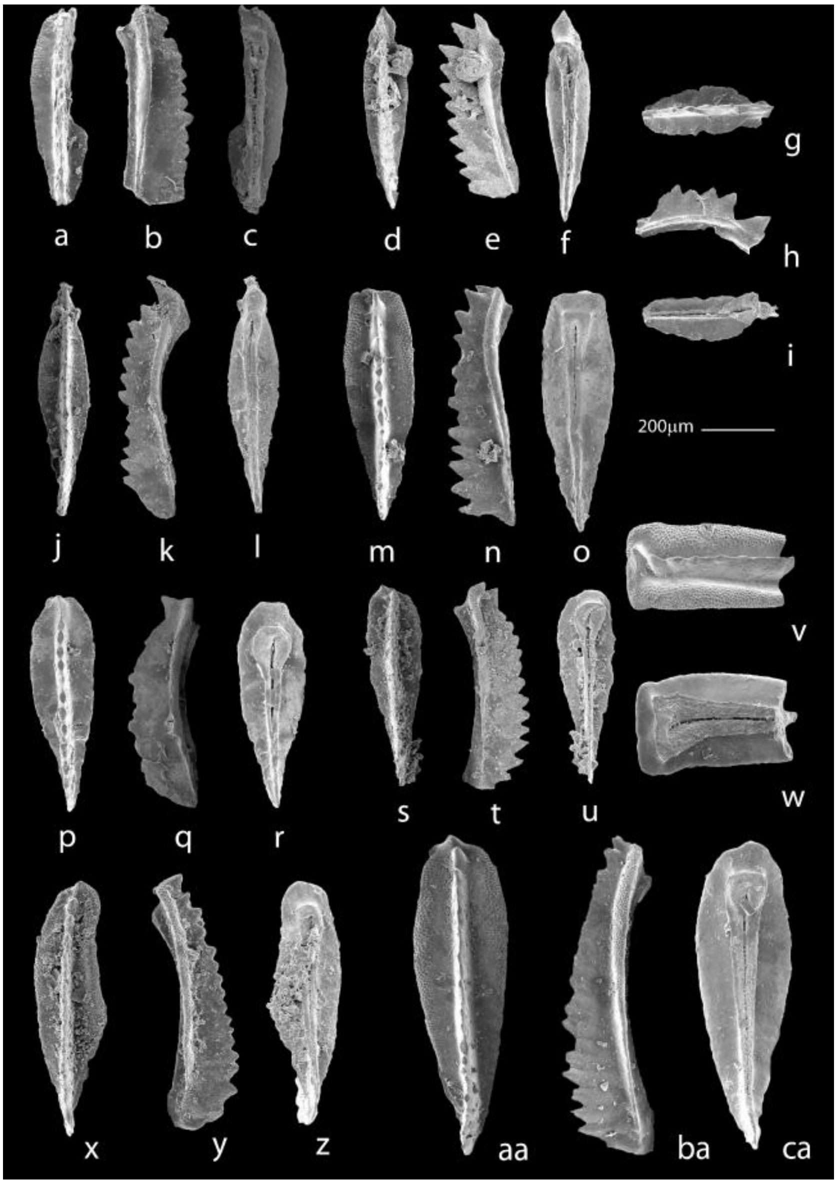

Fig. 6 Conodonts from the Alam Formation, member E. *Neogondolella regale* Mosher transition to *Paragondolella bulgarica* Budurov and Stefanov, sample NK 76, Nakhlak 3 section, (a upper view, b lateral view; c lower view). *Paragondolella bulgarica* Budurov and Stefanov, sample NK 63, Nakhlak 3 section (d juvenile stage, upper view; e juvenile stage, lateral view; f juvenile stage, lower view; g early juvenile stage, upper view; h early juvenile stage, lateral view; i early juvenile stage, lower view). *Neogondolella* cf. *Ng.* constricta cornuta, sample NK 436, Nakhlak 9 section (j upper view; k lateral view; l lower view). *Paragondolella bulgarica* Budurov and Stefanov transition to *Paragondolella hanbulogi* Sudar and Budurov, sample NK 435, Nakhlak 9 section (m upper view; n lateral view; o lower view). *Paragondolella bulgarica* Budurov and Stefanov sample NK 77, Nakhlak 4 section (p upper view; q lateral view; r lower view). *Paragondolella bulgarica* Budurov and Stefanov sample NK 455, Nakhlak 6 section, (s upper view; t lateral view; u lower view). *Paragondolella bifurcata* Budurov and Stefanov sample NK 435, Nakhlak 9 section (v upper view; w lower view). *Paragondolella bulgarica* Budurov and Stefanov, sample NK 455, Nakhlak 6 section (x upper view; y lateral view; z lower view). *Paragondolella bulgarica* Budurov and Stefanov transition to *Paragondolella hanbulogi* Sudar and Budurov, sample NK 435, Nakhlak 9 section (aa upper view; ba lateral view; ca lower view). Scale bar = 200 μm for all pictures.

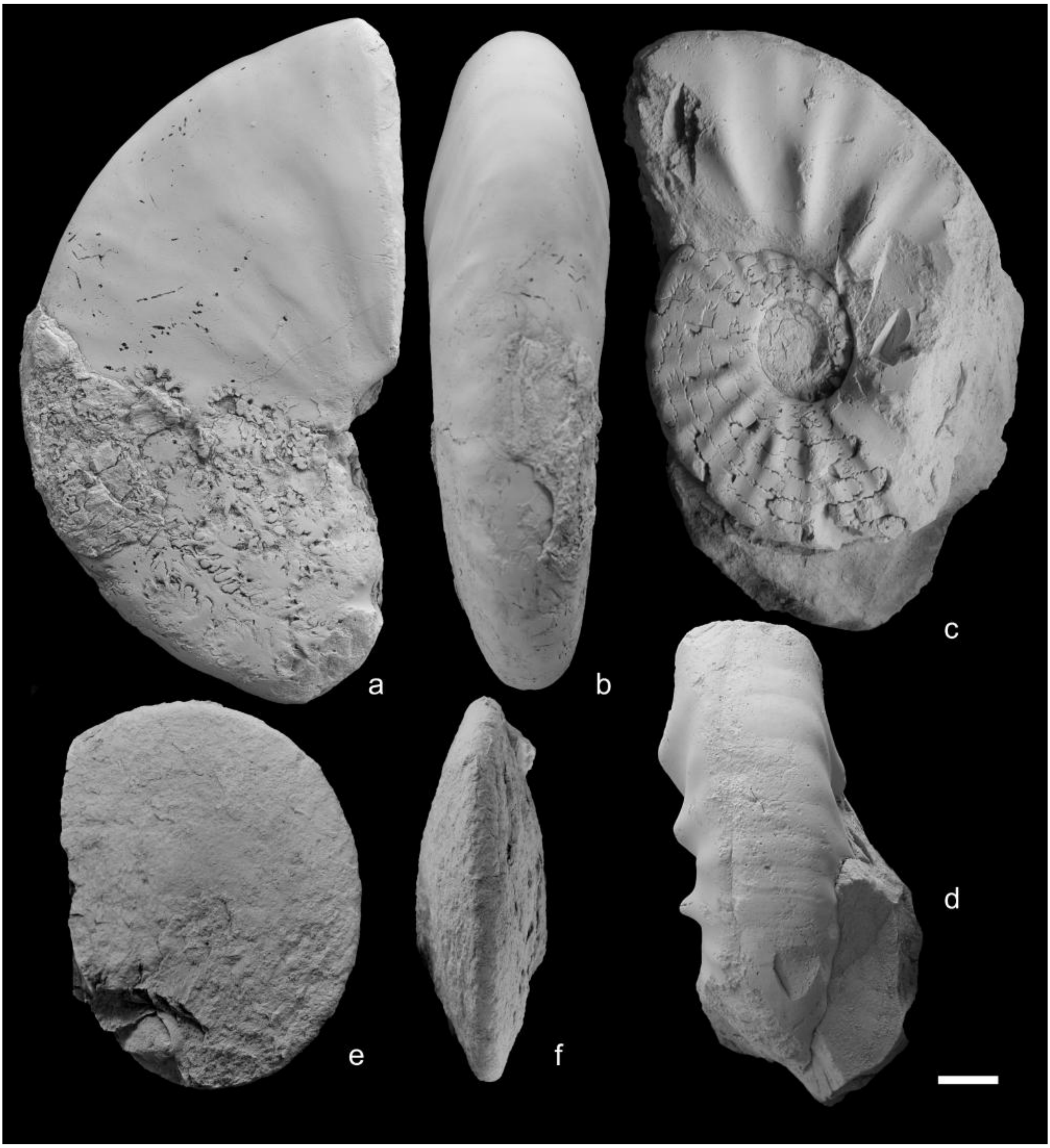

Fig. 7 Late Bithynian ammonoids from the Alam Formation, member E, Nakhlak 6 section, *Aghdarbandites ismidicus* Zone. See Fig. 4 for stratigraphic position of the samples. **a**–**b** *Gymnites asseretoi* Tozer 1972, MPUM 10879 (NK516-2), internal mold. **a** lateral view; **b** ventral view. **c**–**d** *Aghdarbandites ismidicus* (Arthaber 1914), MPUM 10878 (NK516-1), internal mold. **c** lateral view; **d** ventral view. **e**-**f** *Kocaelia toulai* (Arthaber 1914), MPUM 10877 (NK453-15), specimen with test. **e** lateral view; **f** ventral view. Bar scale 1 cm. The specimens are housed at Museo di Paleontologia of Dipartimento di Scienze della Terra “Ardito Desio”, University of Milano. The repository number (MPUM) is given.

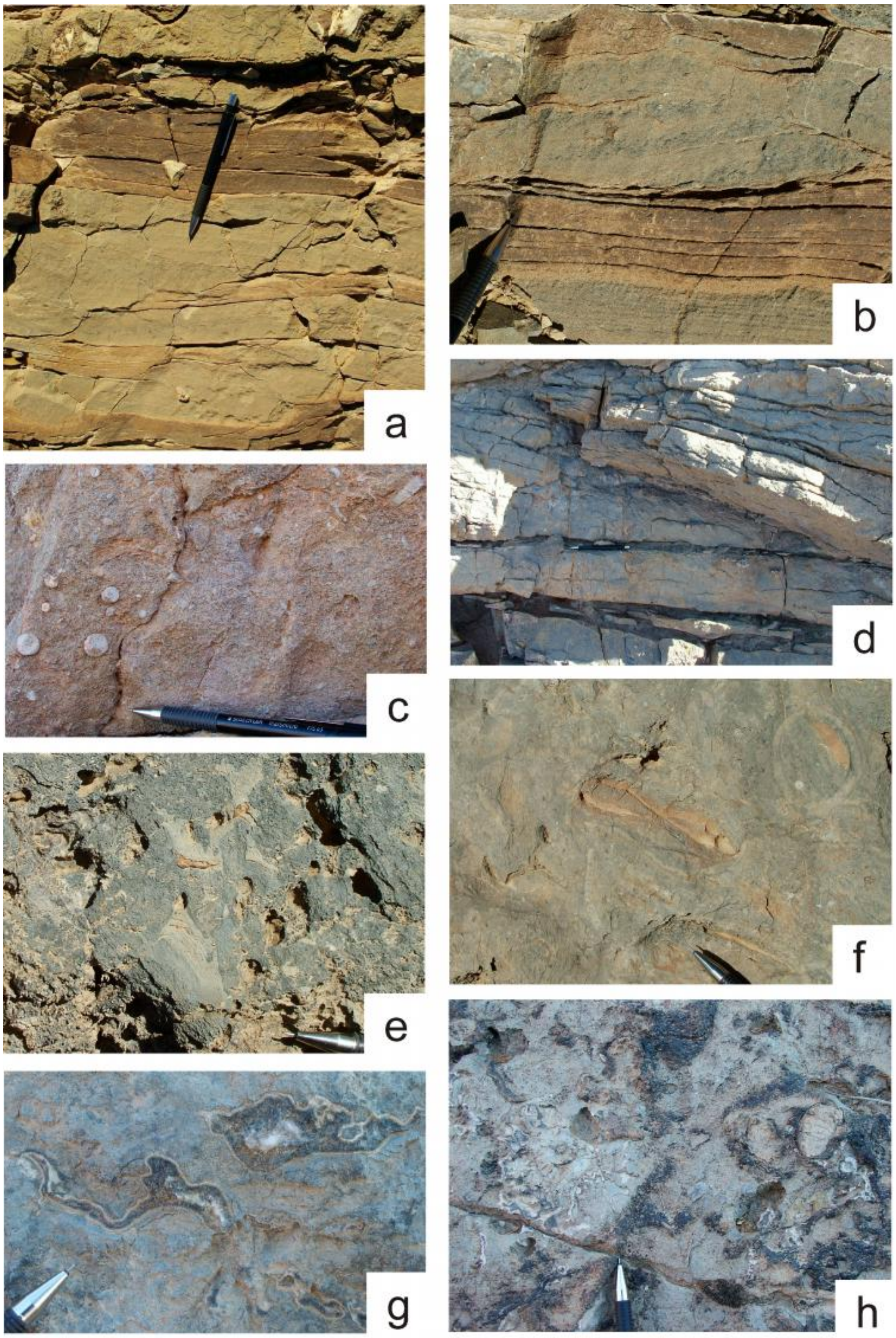

Fig. 8 – Sedimentary structures from different parts of the carbonate mound (F1 to F7 refer to the facies described in the text and in Fig. 9). a) fine grained sandy limestone of the basinal area around and below the carbonate mounds (Facies F6); b) bioclastic limestone and fine-grained sandstones at the toe of the slope of the carbonate mounds (facies F2); c) crinoidal bioclastic packstone from the clinostratified slope of the mounds (facies F1); d) cross lamination in clinostratified bioclastic-intraclastic limestone in the lower part of the slope (pencil for scale; facies F3); e) detail of the massive limestones of the inner part of the mound. Note the presence of light-grey cavities filled by internal sediments (facies F5); f) inner part of the mound with sponge: note the cavities with geopetal filling (facies F5); g) large cavities in the inner part of the mounds filled with spatic cements (facies F5); h) hard ground surface at the top of the mound rich in ammonoids (facies F7).

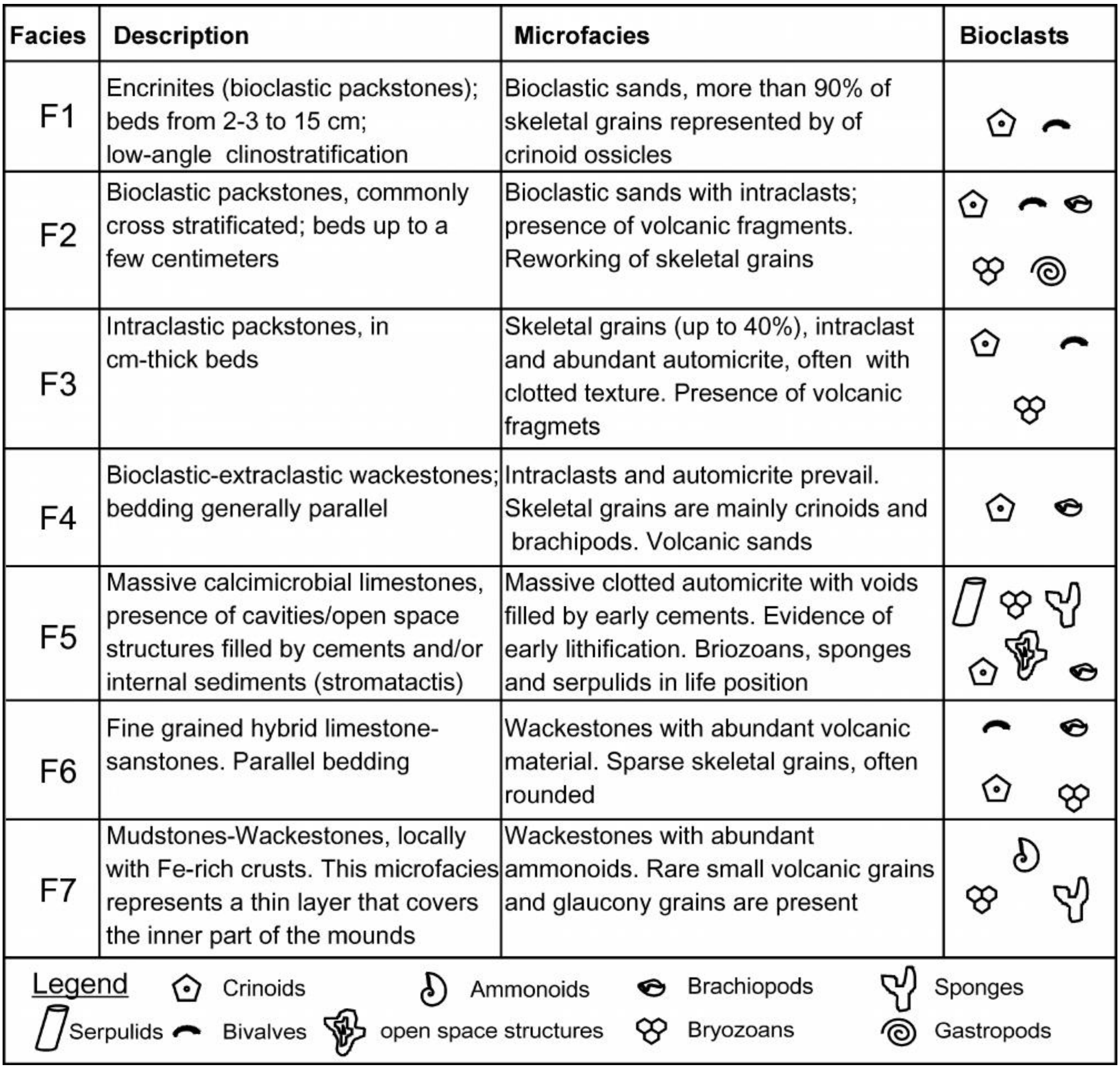

Facies	Description	Microfacies	Bioclasts
F1	Encrinites (bioclastic packstones); beds from 2-3 to 15 cm; low-angle clinostratification	Bioclastic sands, more than 90% of skeletal grains represented by of crinoid ossicles	
F2	Bioclastic packstones, commonly cross stratificated; beds up to a few centimeters	Bioclastic sands with intraclasts; presence of volcanic fragments. Reworking of skeletal grains	
F3	Intraclastic packstones, in cm-thick beds	Skeletal grains (up to 40%), intraclast and abundant automicrite, often with clotted texture. Presence of volcanic fragmets	
F4	Bioclastic-extraclastic wackestones; bedding generally parallel	Intraclasts and automicrite prevail. Skeletal grains are mainly crinoids and brachipods. Volcanic sands	
F5	Massive calcimicrobial limestones, presence of cavities/open space structures filled by cements and/or internal sediments (stromatactis)	Massive clotted automicrite with voids filled by early cements. Evidence of early lithification. Briozoans, sponges and serpulids in life position	
F6	Fine grained hybrid limestone-sanstones. Parallel bedding	Wackestones with abundant volcanic material. Sparse skeletal grains, often rounded	
F7	Mudstones-Wackestones, locally with Fe-rich crusts. This microfacies represents a thin layer that covers the inner part of the mounds	Wackestones with abundant ammonoids. Rare small volcanic grains and glaucony grains are present	

Fig. 9 – Main features of the seven facies recognized in the carbonate mounds and adjoining succession. See text for more details.

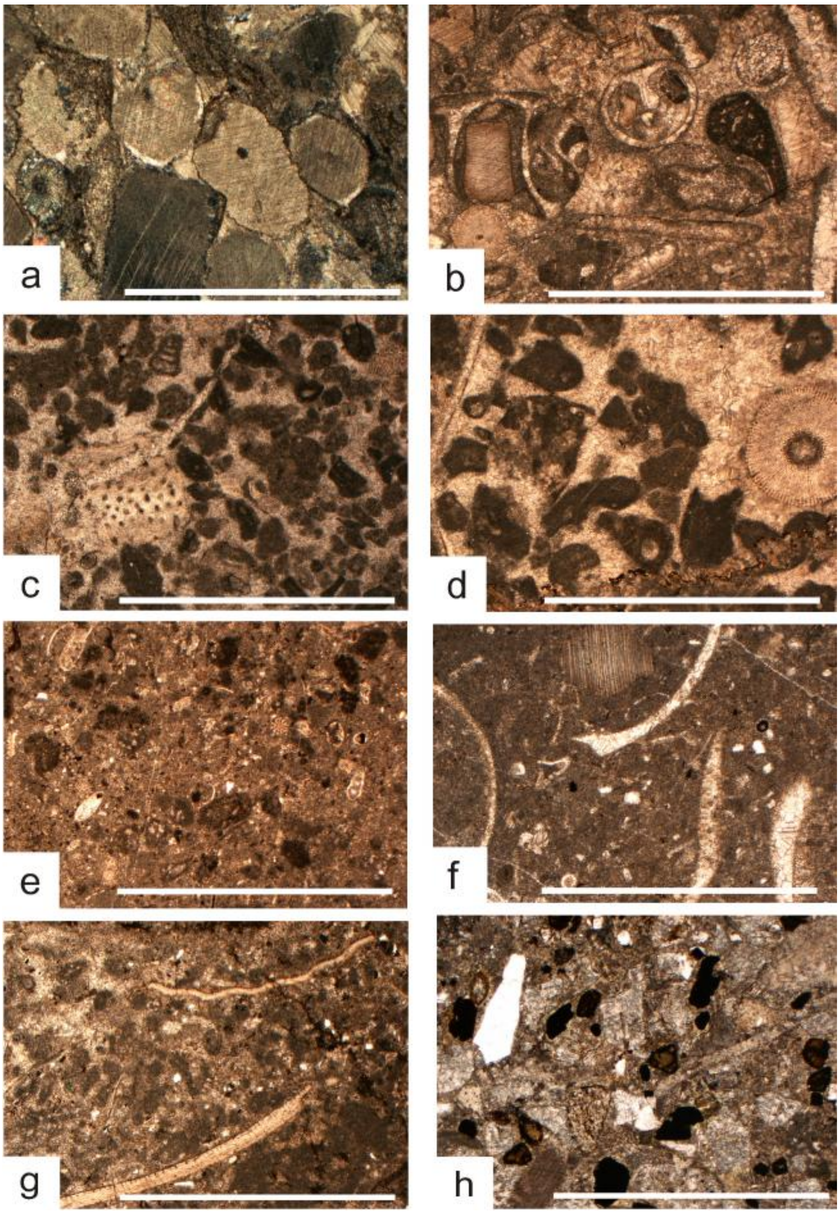

Fig. 10 - Microfacies from the margin, slope and basinal area of the carbonate mounds. a) crinoidal packstone from the upper part of the slope (facies F1, sample NK58); b) bioclastic pakstone with gastropods, bivalves and crinoids. Note the abrasion of the skeletal grains (facies F2, sample NK55); c) intraclastic (automicrite) grainstone with scarce skeletal grains (brachiopods, foraminifera): the intraclasts have a typical clotted texture which denotes the provenance from the inner part of the mound (facies F3, sample KN95); d) another example of intraclastic grainstone, form the slope of the mounds (facies F3; sample NK73); e) basinal wackestone with skeletal grains (a nodosarid can be observed), abundant clotted intraclasts and volcanic extraclasts (distal slope, facies F4, sample NK72 bis); f) example of basinal facies, with crinoids and bivalves in a fine-grained matrix with sparse volcanic grains (facies F6, sample KN69); g) another example of basinal facies, consisting in fine-brained packstone with brachipoids and intraclasts (facies F6,sample NK116); h) condensed facies at the top of the mound: note the presence of abundant volcanic grains and the presence of authigenic minerals (glaucony). Scale bar is 2mm for all the images. Position of samples is shown in Fig. 4.

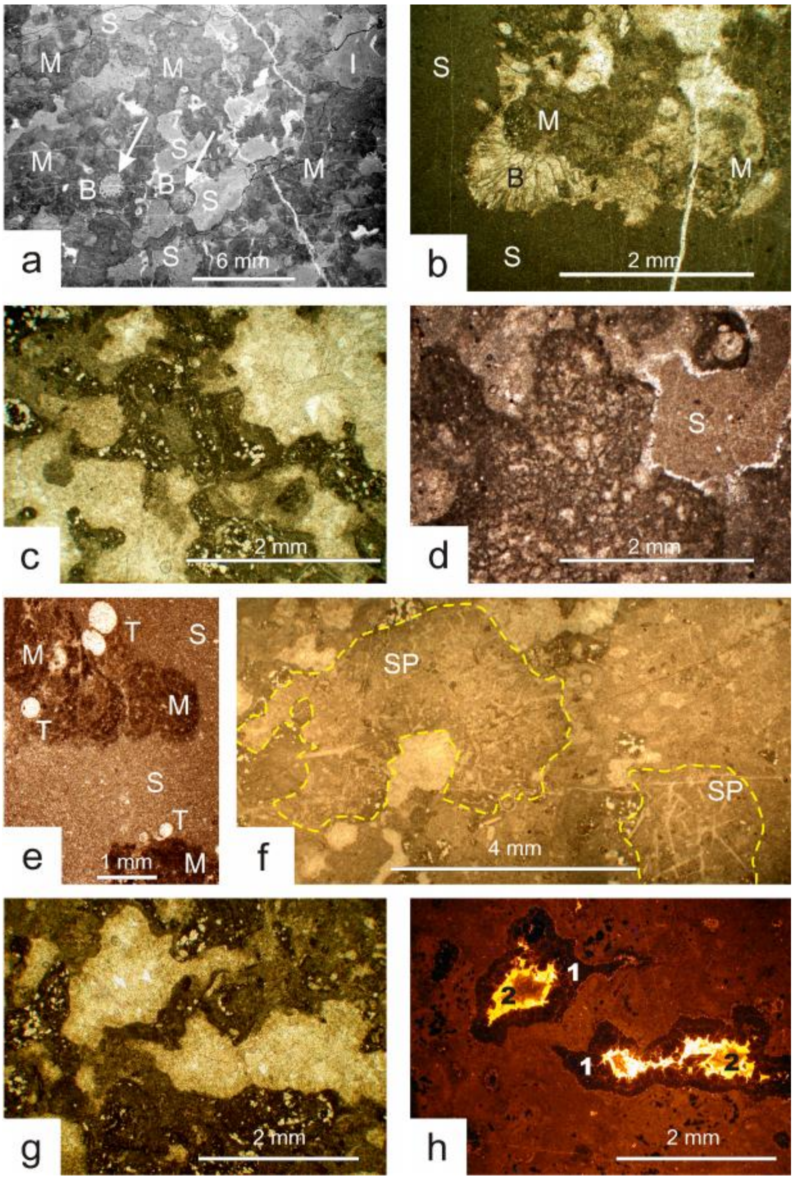

Fig. 11 – Facies and microfacies from the inner part of the mound; a) general aspect of the inner mound microbial limestones (M), with large cavities filled by internal sediments (S). Note the bryozoans (arrows, B) growing on the microbialites (scanned thin section; sample KN84); b) Bryozoan (B) growing on the border of a cavity filled by internal sediments (S). The bryozoan encrusts a firm microbialitic substrate consisting of a clotted texture and *Renalcis*-type crusts (M), with presence of cement-filled cavities, sample KN87; c) microbial crust (*Renalcis*?) creating a highly porous structure with cavities filled by cements (sample KN101), d) microbial structures (*Bacinella irregularis)* in the inner part of the mound. Note the presence of a large cavity filled by internal sediments (S) and the narrow rim of early cements that predate the deposition of the internal sediments (sample KN95); e) microbial limestone (M) enveloping serpulid tubes (T) at the border of a cavity filled by internal sediments (S), sample KN87; f) sponges (SP, surrounded by dashed lines) from the inner mound. Note the preserved spiculae and the presence of cavities filled by cements, sample KN101; g) and h) transmitted (left) and cathodoluminescence (right) images of the cement-filled cavities in the inner part of the mound. Note the dark colour of the early cements which almost completely fill the original voids (1) and the late, luminescent blocky calcite (2) which closes the porosity (sample KN102).

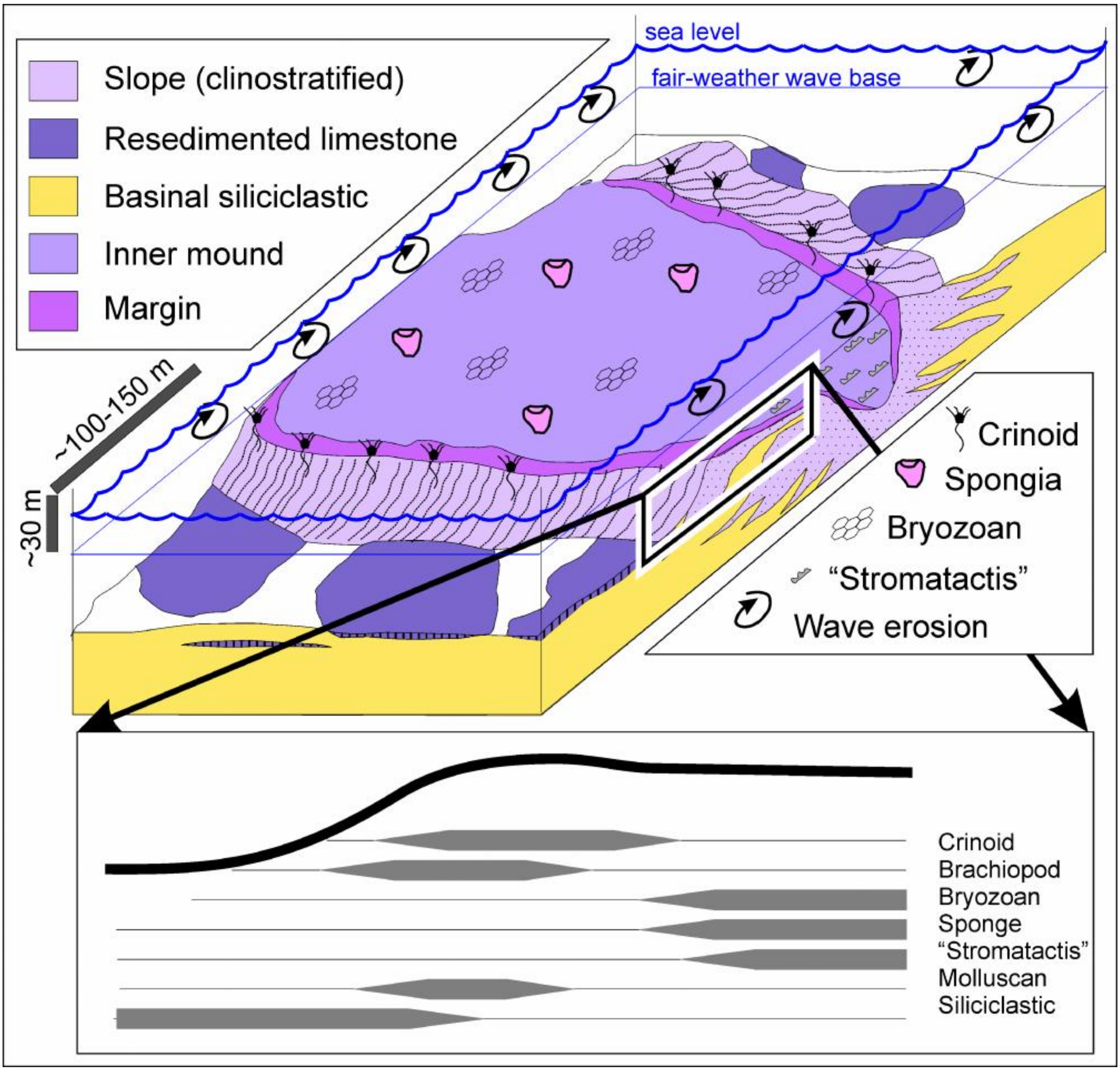

Fig.12 – Depositional model of the carbonate mounds of Nahklak.

References

Alavi M, Vaziri H, Seyed-Emami K, Lasemi Y (1997) The Triassic and associated rocks of the Nakhlak and Aghdarband areas in central and northeastern Iran as remnants of the southern Turanian active continental margin. Geol Soc America Bulletin109:1563- 1575

Angiolini L, Gaetani M, Muttoni G., Stephenson M, Zanchi A 2007 Tethyan oceanic currents and climate gradients 300 m.y. ago. Geology, 35: 1071-1074

Bagheri S, Stampfli GM (2008) The Anarak, Jandaq and Posht-e-Badam metamorphic complexes in central Iran: New geological data, relationships and tectonic implications. Tectonophysics 451:123–155

Balini M, Nicora A, Berra F, Garzanti E, Zanchi A, Levera, M, Zanchetta S, Mossavari F, Rakhmati M (2009) The Triassic of Nakhlak (Central Iran). In: Brunet MF, Wilmsen M, Granath JW (eds) South Caspian to Central Iran Basins. Geological Society of London Special Publications 312:287-321

Balini M, Lucas SG, Jenks JF, Spielmann JA (2010) Triassic ammonoid biostratigraphy: an overview. In: Lucas S.G. (ed.) The Triassic Timescale. Geological Society of London Special Publication, 334, 221-264

Berra F, Rettori R, Bassi D (2005) Recovery of carbonate platform production in the Lombardy Basin during the Anisian: paleoecological significance and constrain on paleogeographic evolution. Facies 50:615-27

Brayard A, Vennin E, Olivier N, Bylund KG, Jenks J, Stephen DA, Bucher H, Hofmann R, Goudemand N, Escarguel G (2011) Transient metazoan reefs in the aftermath of the end-Permian mass extinction. Nature Geoscience, DOI: 10.1038/NGEO1264

Davoudzadeh M, Seyed-Emami K (1972) Stratigraphy of the Triassic Nakhlak Group, Anarak region, Central Iran. Geol Surv Iran, Report 28:5-28, Tehran

Fantini Sestini N (1988) Anisian ammonites from Gebze area (Kokaeli peninsula, Turkey. Riv Ital Paleont Strat, 94; 35-80

Fantini Sestini N (1990) *Kocaelia* gen. n. (Family Beyrichitidae) from Middle Anisian. Riv Ital Paleont Strat 95:343-350

Flügel E (2004) Microfacies of carbonate rocks. Analysis, interpretation and application. Springer, Berlin

Flügel E, Stanley GD Jr (1984) Reorganization, development and evolution of post-Permian reefs and reef organisms. Palaeontographica Americana 54:177–186

Germani D (2000) Conodonti dell'Anisico medio nella Tetide occidentale: Tassonomia, biostratigrafia e filogenesi. Tesi di dottorato, University of Milano

Hips K (2007) Facies pattern of western Tethyan Middle Triassic black carbonates: The example of Gutenstein Formation in Silica Nappe, Carpathians, Hungary, and its correlation to formations of adjoining areas. Sedimentary Geology 194:99–114

Holzer, HF, Ghasemipour R (1973) Geology of the Nakhlak Lead Mine area (Anarak District, central Iran). Geol Surv Iran Report 21:5–26

Keim L, Schlager W (2001) Quantitative compositional analysis of a Triassic carbonate platform (Southern Alps, Italy). Sedimentary Geology 139:261-283

Kiessling W (2010) Reef expansion during the Triassic: Spread of photosymbiosis balancing climatic cooling. Palaeogeogr Palaeoclimatol Palaeoecol 290, 11-19

Kovacs S, Ralisch-Felgenhauer E (2005) Middle Anisian (Pelsonian) platform conodonts from the Triassic of the Mecsek Mts (South Hungary) Their taxonomy and stratigraphic significance. Acta Geol Hungarica 48:69-105

Krystyn L, Balini M, Nicora A (2004) Lower and Middle Triassic stage and substage boundaries in Spiti. Albertiana 30:39-52

Lehrmann D J (1999) Early Triassic calcimicrobial mounds and biostromes of the Nanpanjiang basin, south China. Geology 27:359–362

Lehrmann DJ, Wei JY, Enos P (1998) Controls on facies architecture of a large Triassic carbonate platform: the Great Bank of Guizhou, Nanpanjiang Basin,South China. Journal of Sedimentary Research 68: 311–326

Morycowa E (1988) Middle Triassic Scleractinia from the Cracow-Silesia region, Poland. Acta Palaeontol Polonica 33:91-121

Mounji D, Bourque PA, Savard MM (1998) Hydrothermal origin of Devonian conical mounds (kess-kess) of Hamar Lakhdad Ridge, Anti-Atlas, Morocco. Geology 26:1123–1126

Mundil R, Palfy J, Renne PR, Brack P (2010) The Triassic time scale: new constraints and a review of geochronological data. In: Lucas SG (ed.) The Triassic Timescale. Geological Society London Special Publications, 334:41–60

Muttoni G, Mattei M, Balini M, Zanchi A, Gaetani M, Berra F (2009) The drift history of Iran from the Ordovician to the Triassic. In: Brunet MF, Wilmsen M, Granath JW (eds) South Caspian to Central Iran Basins. Geological Society London Special Publications 312:7–29

Neri C, Gianolla P, Furlanis S, Caputo R, Bosellini A (2007) Note Illustrative della Carta Geologica d'Italia alla scala 1:50.000, Foglio 029 Cortina d'Ampezzo. A.P.A.T. SystemCart, Roma, 200 pp

Orchard MJ, Lehrmann DJ, Jiayong W, Hingmei W, Taylor HJ (2007) Conodonts from the Olenekian.Anisian boundary beds, Guandao, Guizhou Province, China. In: Lucas SG, Spielmann JA (eds.) The Global Triassic. New Mexico Museum of Natural History and Science Bulletin, 41:347-354

Payne JL, Lehrmann DJ, Christensen S, Wei J, Knoll AH (2006a) Environmental and biological controls on the initiation and growth of a Middle Triassic (Anisian) reef complex on the Great Bank of Guizhou, Guzhou Province, China. Palaios, 21:325–343.

Payne JL, Lehrmann DJ, Wei J, Knoll AH (2006b) The Pattern and Timing of Biotic Recovery from the End-Permian Extinction on the Great Bank of Guizhou, Guizhou Province, China. Palaios 21:63–85

Playford PE (1984) Platform-margin and marginal slope relationships in Devonian reef complexes of the Canning Basin. In: Parcell PG (Ed.), The Canning Basin W.A. Proceedings of Geological Society of Australia/ Petroleum Exploration Survey of Australia, Canning Basin Symposium Perth 189–215

Riding R (2000) Microbial carbonates: the geological record of calcified bacterial-algal mats and biofilms. Sedimentology 47:179–214

Riding R, Liang L (2005) Geobiology of microbial carbonates: metazoan and seawater saturation state influences on secular trends during the Phanerozoic. Palaeogeogr Palaeoclimatol Palaeoecol 219:101–115

Schlager, W (2003) Benthic carbonate factories of the Phanerozoic. Int J Earth Sci (Geol Rundsch) 92:445–464

Senowbari-Daryan B, Zühlke R, Bechstädt T, Flügel E (1993) Anisian (Middle Triassic) buildups of the northern Dolomites (Italy): The recovery of reef communities after the Permian/ Triassic crisis. Facies 28:181–256

Seyed-Emami K. (2003) Triassic of Iran. Facies 48:91–106

Sharkovski M, Susov M, Krivyakin B (1984) Geology of the Anarak Area (Central Iran). Explanatory Text of the Anarak Quadrangle Map 1:250 000. Geol Surv Iran 1–143

Shen J-W, Webb G.E., Jell J.S (2008) Platform margins, reef facies, and microbial carbonates; a comparison of Devonian reef complexes in the Canning Basin, Western Australia, and the Guilin region, South China. Earth Science Reviews 88:33-59

Soffel H, Davoudzadeh M, Rolf C, Schimdt S (1996) New paleomagnetic data from Central Iran and a Triassic paleoreconstruction. Geol Rundsch 85:293-302

Stanley DG (2003) The evolution of modern corals and their early history. Earth-Sci Rev 60:195–225

Stefani M, Furin S, Gianolla P (2010) The changing climate framework and depositional dynamics of Triassic carbonate platforms from the Dolomites. Palaeogeogr Palaeoclimatol Palaeoecol 290:43–57

Tozer ET (1972) Triassic ammonoids and Daonella from the Nakhlak Group, Anarak region, Central Iran. Geol Sur Iran Report 28:29–69

Webb GE (2001) Famennian mud-mounds in the proximal fore-reef slope, Canning Basin, Western Australia. Sedimentary Geology 145:295–315

Wendt J, Kaufmann B, Belka Z (2001) An exhumed Palaeozoic underwater scenery; the Visean mud mounds of the eastern Anti-Atlas (Morocco). Sedimentary Geology 145:215–233

Zanchi A, Zanchetta S, Garzanti E, Balini M, Berra F, Mattei M, Muttoni G (2009) The Cimmerian evolution of the Nakhlak–Anarak area, Central Iran, and its bearing for the reconstruction of the history of the Eurasian margin. In: Brunet MF, Wilmsen M, Granath JW (eds) South Caspian to Central Iran Basins. Geological Society London Special Publications 312:261–286